MICHIGAN RADIOLOGICAL SOCIETY
RESIDENT & FELLOW SECTION

17th Annual Resident Research Forum

ABSTRACT BOOKLET

May 4, 2024
Baronette Renaissance,
Novi, MI

AGENDA

27TH ANNUAL RESIDENT SECTION CONFERENCE & 17TH ANNUAL RESIDENT RESEARCH FORUM

FRIDAY, MAY 3, 2024

10:00 AM	Registration & Breakfast
10:50 AM	Introduction
11:00 AM	Daniel Corbett, Radiology Business Solutions
12:00 PM	Lunch
1:00 PM	Angel A Gómez-Cintrón, M.D.
2:00 PM	Abstract Presentations
2:50 PM	Break with Sponsors
3:10 PM	Speaker Panel -
	Kenneth Buckwalter, MD, MBA, FACR (U of M)
	Randy Hicks, MD, MBA, FACR (RMI)
	Chad Klochko, MD (HFH)
	Karen Grazjewski, MD (HVR)
	Michael Kasotakis, MD (HVR)
	Andrew Moriarity, MD (ARS)
3:40 PM	Quiz Bowl - University of Michigan
4:10 PM	Announcement of 2023 Board Members
4:40 PM	Adjourn
5:00 PM	Networking Reception

ANGEL A GÓMEZ-CINTRÓN, M.D.

Diagnostic Radiology Residency Program Director
UT Health San Antonio.
San Antonio, TX

Dr. Gómez-Cintrón is a musculoskeletal radiologist with special interest in image guided interventions, education and inclusion. Dr. Gómez-Cintrón also serves as the Diagnostic Radiology residency program director. He completed his medical school and radiology residency at the University of Puerto Rico, before MSK fellowship training at UT Health San Antonio. After fellowship, Dr. Gómez-Cintrón returned to the University of Puerto Rico as the residency program director and Body Imaging section chief. After five years, Dr. Gómez-Cintrón moved to The University of Alabama at Birmingham where he served as the section chief of the MSK section, director of MRI and associate residency program director. In 2017, Dr. Gómez-Cintrón returned to UT Health San Antonio. You can find Dr. Gómez-Cintron in the CT procedure room, actively participating in medical education, mentoring medical students or in the reading room.

17TH ANNUAL RESIDENT RESEARCH FORUM ABSTRACT SUBMISSIONS

ABSTRACT WINNERS

Diagnostic/Interventional:

Kirti Dhingra, DO
Ascention Providence
Radiologist Accuracy in Predicting Pahtology In Breast Imaging

Richard Pearson, MD,
Corewell Health- West
Impact of a Common Interpretation Platform on Pediatric Imaging

Radiation Oncology:

Joseph Lee, MD,
Corewell, Beaumont, Royal Oak
Prognostic Value of MRI-Assessed Central Gland Volume for Biochemical Recurrence after Prostate Radiotherapy

Samuel Regan, MD,
University of Mchigan
FDG-PET-based Selective De-escalation of Radiotherapy for HPV-Related Oropharynx Cancer: Results from a Phase II Trial

Medical Students:

Joshua Baker,
Michigan State University
Insights of Contemporary Diffusion MRI Modeling Techniques in Mild Traumatic Brain Injury: A TRACK-TBI Study

Haniyeh Zamani,
Wayne State University/Detroit Medical Center
Recovery and Adaptation: Radiology Volumes Post-Pandemic Using Data from 12.4 Million Imaging Examinations, 197 Facilities, and 1,600 Radiologists

Radiologist Accuracy in Predicting Pathology of Breast Imaging

Authors: **Kirti Dhingra, DO, PhD**, Jeff Lin, MD, Grace Brennan, MD, Nedi Gari, MD, Evita Singh, MD

Purpose: Breast cancer, the most prevalent cancer in women and second only to lung cancer in female mortality, has seen rising incidence, especially during the 1980s and 1990s due to increased mammography screening. Screening's primary goal is early tumor detection, reducing mortality by over 20%. Yet, it has downsides, including false-positive results leading to unnecessary benign biopsies and patient anxiety.

In the UK, 69% of false positives undergo additional imaging, with 31% requiring biopsies. In Canada, the expected malignant rate among women needing breast biopsies falls between 30-50%. In the UK and the US, 2.3-3.4% of initial screening mammograms and 0.8-1.7% of follow-up ones lead to breast biopsies. Approximately 5-10% of screening mammograms reveal abnormalities, with most not indicative of cancer.

The proliferation of image-guided breast biopsies has raised concerns about their frequency. Radiologists' experience also influences biopsy recommendations. A radiologists' ability to predict breast histology from imaging findings remains an understudied domain.

This study's core purpose is to comprehensively analyze the ability of a radiologist to predict benign versus malignant results to provide guidance in reducing the number of benign biopsies..

Materials and Methods

This prospective study involved radiologists completing survey sheets when recommending biopsies and when performing the biopsy, predicting benign vs malignant, specific pathology, with confidence interval. Predictions were compared to the final biopsy results to determine accuracy. All patients who underwent biopsy at our institutions were included in the data. Data was categorized as either concordant or discordant when comparing predicted pathology results to actual.

Results

The accuracy of radiologist prediction from initial diagnostic imaging when compared to actual pathology results in the study population is 69.47% (95% CI,59.18%-78.51%) with a sensitivity of 75.68% (95% CI, 58.80%-88.23%). The accuracy of biopsy imaging when compared to actual pathology results in this population is 80% (95% CI, 70.54%-87.51%) with sensitivity of 78.38% (95% CI, 61.79%-90.17%). Highly experienced breast radiologists tend to perform better at prediction 80.8% (70.3-80.2 CI) compared to moderately experienced at 76.5 % (50.1-93.2%).

Conclusion

The preliminary data indicates that radiologists are very good at predicting the pathology based imaging features. The radiologists that practice breast imaging primarily or radiologists who have incurred years of experience are more accurately able to predict pathology.

Clinical Relevance Statement (50 words max)

This data will potentially help radiologists gain confidence in watching based on imaging features (BIRADS 3) to reduce benign biopsies.

Main Pancreatic Duct Stone Presenting with Acute Focal Pancreatitis

Roham Hadidchi, **Shahram Hadidchi MD**, Michael Burcescu MD
Department of Radiology, Detroit Medical Center, Wayne State University, Detroit, USA.

Introduction

A pancreatic stone is a solid formation of calcium salts and proteins that can develop in the pancreatic ducts [1,2]. They can vary in size and cause blockages or obstruction in the pancreatic ducts, leading to complications such as acute pancreatitis, abdominal pain, digestive difficulties, and sometimes infection. Chronic pancreatitis and excessive alcohol consumption are the most common causes of pancreatic stones [3]. In this study, we

Case Presentation

Patient was a 36-year-old male patient with history of alcohol use disorder and previous episodes of alcohol related acute pancreatitis presented to the emergency department for epigastric abdominal pain with radiation towards his back in the setting of nausea and vomiting. He denies any fevers, chills, or diarrhea. Patient stated that he is a current smoker and used to drink a lot of hard liquor on the weekends. On physical exam he had significant abdominal tenderness primarily in the epigastrium with no right upper quadrant tenderness, CVA tenderness, guarding or rigidity. Labs showed elevated ALT: 84 Units/Liter (normal range 7-52) and AST: 44 Units/Liter (normal range 13-39), consistent with the patient's history of alcohol use disorder. Lipase was elevated at 341 Units/Liter (normal range 11-82). CT abdomen/pelvis was performed and showed a 5 mm calcified stone in the main pancreatic duct with upstream dilatation of the duct and pancreatic and peripancreatic edema along the body and tail of the pancreas. Findings were compatible with obstructive main pancreatic duct stone resulting in focal acute pancreatitis of the body and tail of the pancreas. Ultrasound of the upper abdomen was also performed and demonstrated a subcentimeter echogenic focus in the body of the pancreas with posterior shadowing and twinkle artifact, corresponding to findings on the CT abdomen, compatible with main pancreatic duct stone.

Discussion

The main cause of pancreatic stone formation is the presence of high concentrations of calcium or other minerals in the pancreatic ducts, leading to the formation of solid deposits over time [4]. This can be associated with conditions such as chronic pancreatitis, where inflammation and damage to the pancreas can alter the composition of pancreatic secretions [4]. Other contributing factors may include a history of recurrent pancreatitis, genetic predisposition, certain medications, metabolic disorders like hyperparathyroidism, or anatomical abnormalities in the pancreas or its ducts [5]. Additionally, excessive alcohol consumption may also play a role in the development of pancreatic stones [4].

Pancreatic stones can be visualized in abdominal imaging studies including CT, MRI, transabdominal ultrasound, or endoscopic ultrasound (EUS). On CT, pancreatic stones appear as dense, opaque structures within the pancreatic ducts [6]. MRI can also detect pancreatic stones, showing them as signal voids or areas of low signal intensity on T1 and T2 images [7]. In transabdominal ultrasound, the pancreatic stone appears as an echogenic focus with posterior shadowing and occasionally twinkle artifact. EUS is particularly effective for detecting smaller pancreatic stones that may not be clearly visible on other imaging modalities [8].

There are medical, endoscopic, and surgical approaches to the management of pancreatic stones. A low fat diet decreases the release of cholecystokinin, lowering pancreatic secretion and reducing hydrostatic pressure. Oral supplements of pancreatic enzymes and analgesics are also used. Endoscopic treatments include endoscopic sphincterotomy, and extraction. Surgery is considered the second line of management for patients that endoscopic therapy is not effective [9].

Imaging of Traumatic Lung Injury

Authors: **Max Ofori, MD**, Gulchin Altinok, MD

Residency: Detroit Medical Center/Wayne State Diagnostic Radiology

Introduction:
Mortality rate with blunt chest trauma can be as high as 60%, and 20-25% of deaths in polytrauma can be due to chest injury. It is crucial to recognize the types of acute traumatic chest wall injuries timely.

Methods:
We reviewed the imaging studies of the trauma patients and excluded cardiac emergencies to study lung injury types and characteristic imaging findings to avoid diagnostic pitfalls.

Results:
All of the trauma patients had an initial chest radiograph, that usually showed some indications of underlying chest wall or lung injuries, such as: pulmonary contusions, rib fractures, pleural effusions, hemothorax or abnormal air collections, like pneumothorax, pneumomediastinum, pneumopericardium or diaphragmatic tear.

Conclusion:
Complications associated with location and increased number of the rib fractures included flail chest, type 3 lung laceration, hepatic and splenic lacerations in addition to mediastinal injuries associated with high impact first rib fractures.

Impact of a Common Interpretation Platform on Pediatric Imaging

Authors: Jamie Frost, DO; Joseph Junewick, MD; and **Richard Pearson, MD**

Corewell Health- West Diagnostic Radiology Resident Program

Introduction:
Historically, access to subspecialty radiologist interpretations has demonstrated a rural-urban divide which has been even more pronounced in pediatric radiology. A dramatic rise in teleradiology services accelerated by the Covid-19 pandemic has shifted this paradigm. Although access has improved, notable barriers to the availability of subspecialty radiology interpretation remain. This study explores the effects of a common interpretation platform on access to pediatric radiology subspecialist interpretations.

Methods: We present a retrospective study of pediatric radiology examinations at a large private multi-specialty practice servicing several hospital systems in Michigan. Studies for patients under 18 years of age were identified by billing audit. Interventional and mammographic codes were excluded. Studies were divided into 3 timeframes: before, during, and after transition to a common integrated EMR-PACS platform. The percentage of total studies interpreted by pediatric subspecialty radiologists and average turn-around time (time from upload of the study to signing of the report) were calculated for these timeframes.

Results: A total of 288,287 examinations met inclusion criteria. At the children's hospital, 84.4% of studies were interpreted by pediatric radiologists during the baseline timeframe compared to 91.2% after the transition was complete. At the other covered hospitals, 38.9% of studies were interpreted by pediatric radiologists during the baseline timeframe compared to 73.8% after the transition was complete. These increased percentages correlated with a 375% increase in the absolute number of studies read by pediatric radiologists. These increased percentages also correlated with improved turn-around time for study interpretation by 03:24:36 during the same timeframes. In summation, implementation of a common imaging interpretation platform resulted in significantly improved access to pediatric radiology subspecialty interpretation of pediatric studies and improved turn-around time for those interpretations.

Conclusions: Our study demonstrates that implementation of a common interpretation platform provides scalable opportunity for improvements in access and turn-around time for specialized pediatric radiology coverage. Transitioning to a such a platform would be expected to result in improvements in the same metrics in other radiological subspecialties as well.

Beyond the Sinuses: Radiologic Findings of Sinusitis-Related Intracranial Complications

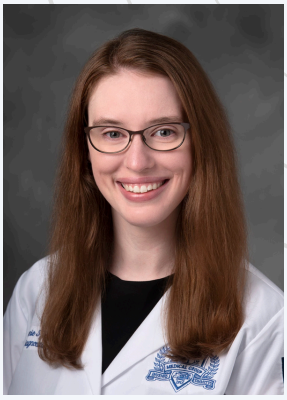

Authors: **Stephanie Szczesniak, M.D.** and Daniel Noujaim, M.D.

Henry Ford Health System

Introduction:

Intracranial complications from sinusitis are rare, but potentially fatal, and are important for radiologists to identify on cross-sectional imaging to guide treatment plans. Our educational exhibit will discuss the various etiologies of paranasal sinus infections, as well as the epidemiology related to susceptible populations. We will then discuss the relevant paranasal sinus anatomy and the routes of intracranial extension, such as direct and venous spread. Then, our educational exhibit will discuss the CT and MRI findings of sinusitis and the secondary intracranial complications (Figs. 1-4). With each case of sinusitis with intracranial extension presented, a multidisciplinary treatment plan will be discussed, including medical and surgical components. The purpose of our educational exhibit is to provide a review of the imaging features of sinusitis-related intracranial sequelae and to highlight the role of the radiologist within the multidisciplinary treatment team.

Figures Demonstrating Intracranial Sequelae of Sinusitis:

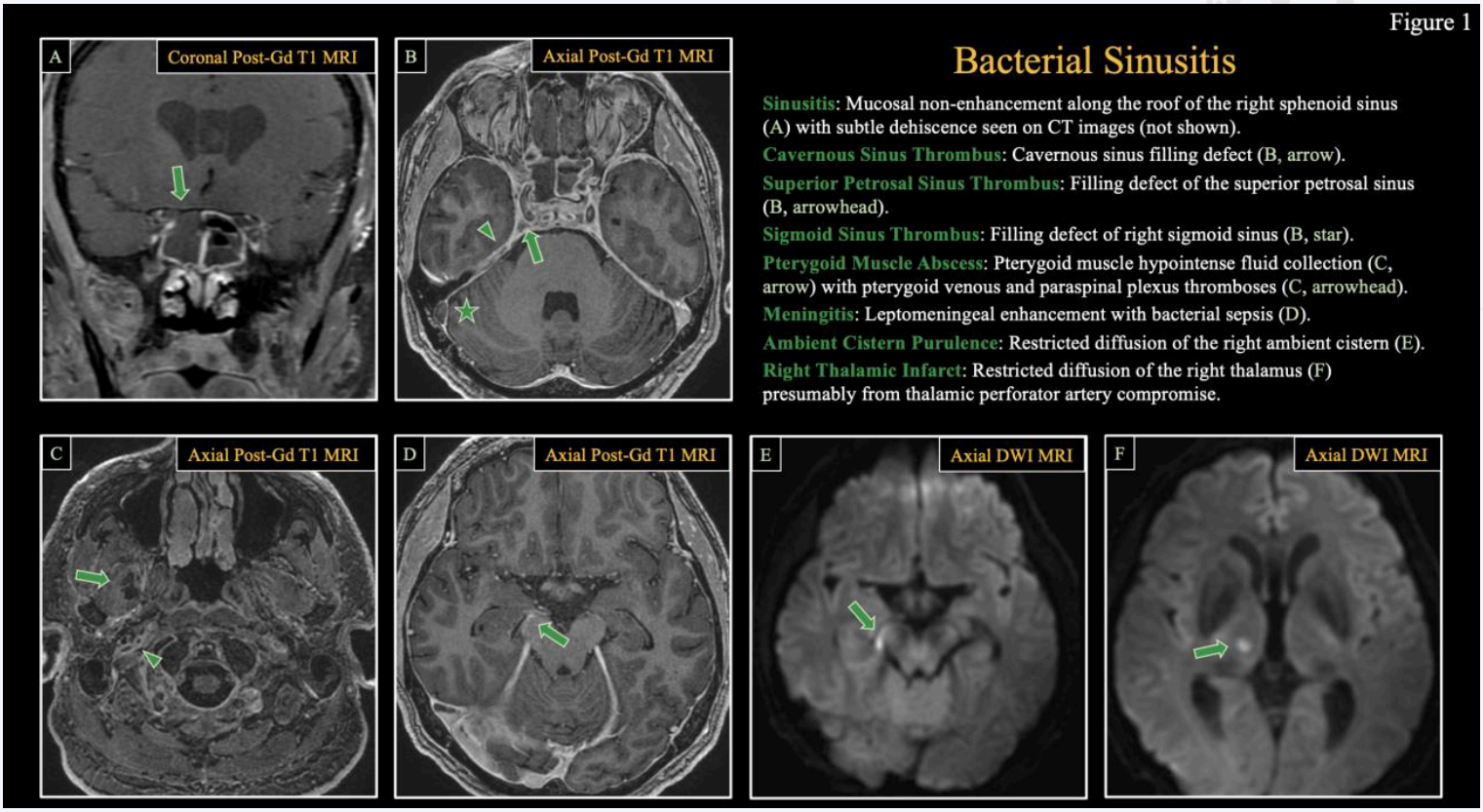

Figure 1 – Bacterial Sinusitis: 52-year-old male with a recent upper respiratory infection who presented with headache and ataxia and was found to have bacterial meningitis on lumbar puncture. Patient underwent functional endoscopic sinus surgery (FESS) with otolaryngology and made a good recovery after completing intravenous antibiotics

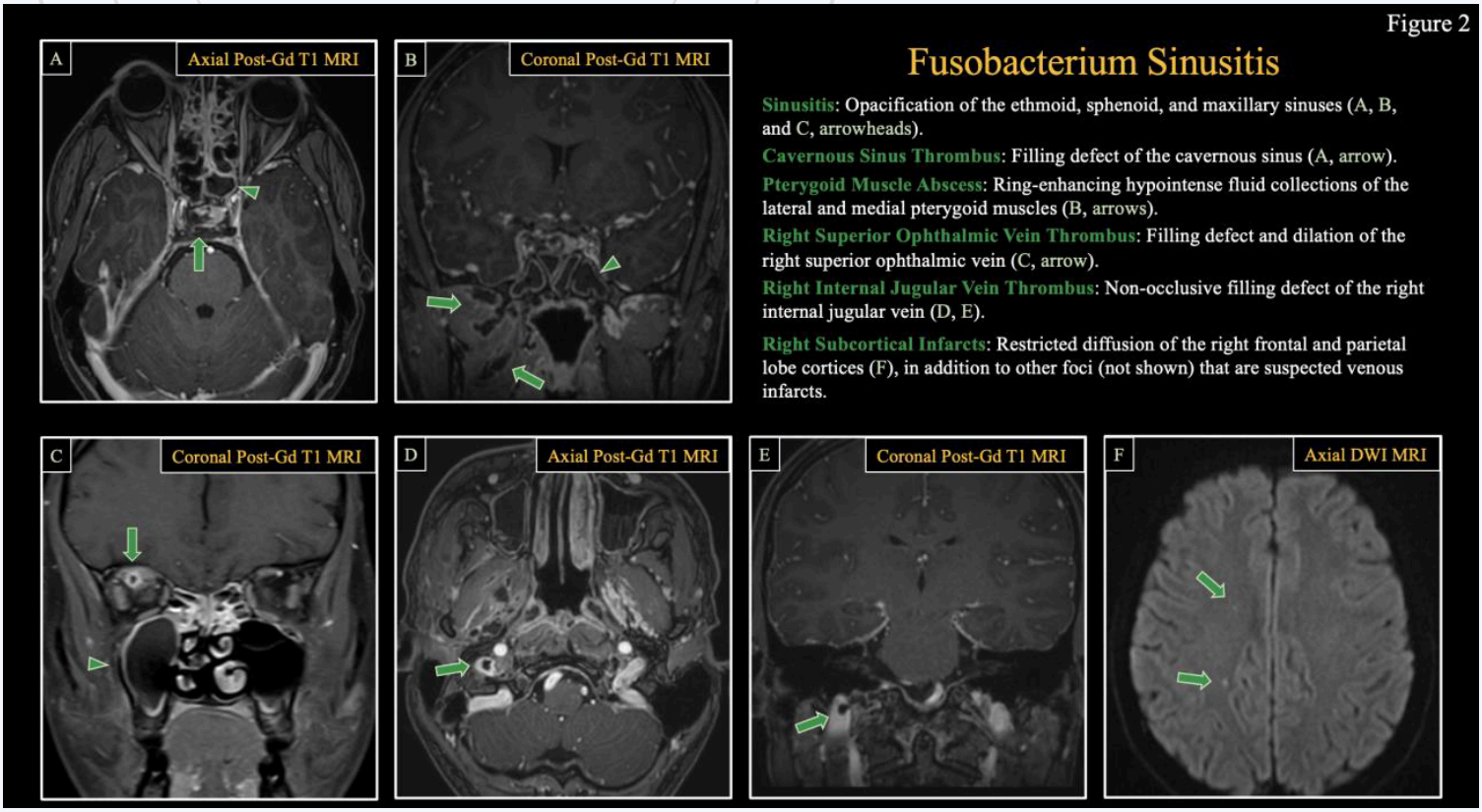

Figure 2 – Fusobacterium Sinusitis: 20-year-old male with recent upper respiratory infection who presented with worsening facial pain and was found to have Fusobacterium necrophorum bacteremia. Patient underwent treatment with intravenous antibiotics and made a good recovery.

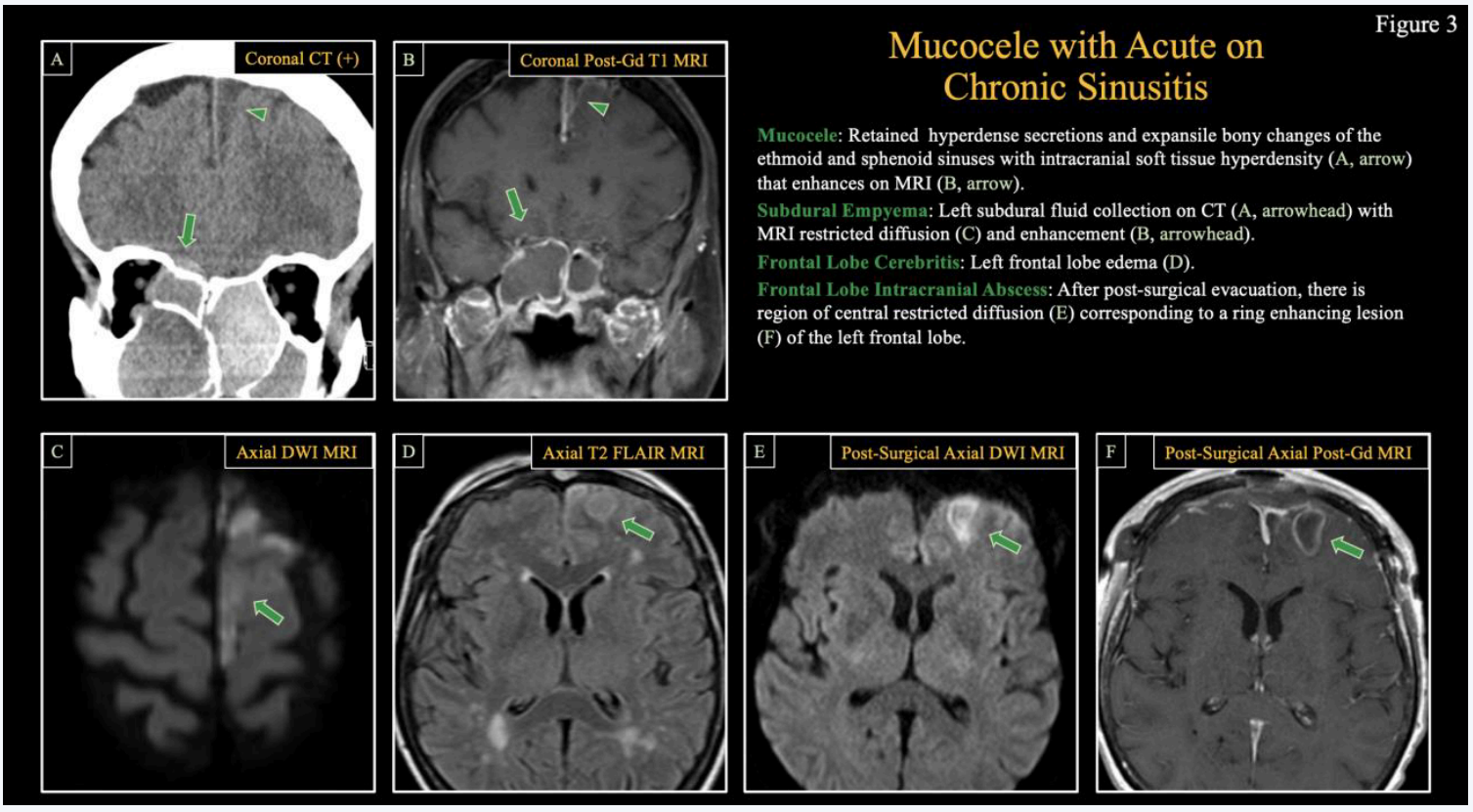

Figure 3 – Mucocele with Acute on Chronic Sinusitis: 73-year-old female with recurrent sinus infections secondary to nasal polyps who presented with lethargy and seizures and was found to have bifrontal abnormalities on EEG. Patient made a good recovery undergoing FESS and bifrontal craniotomy and evacuation and was treated with intravenous antibiotics.

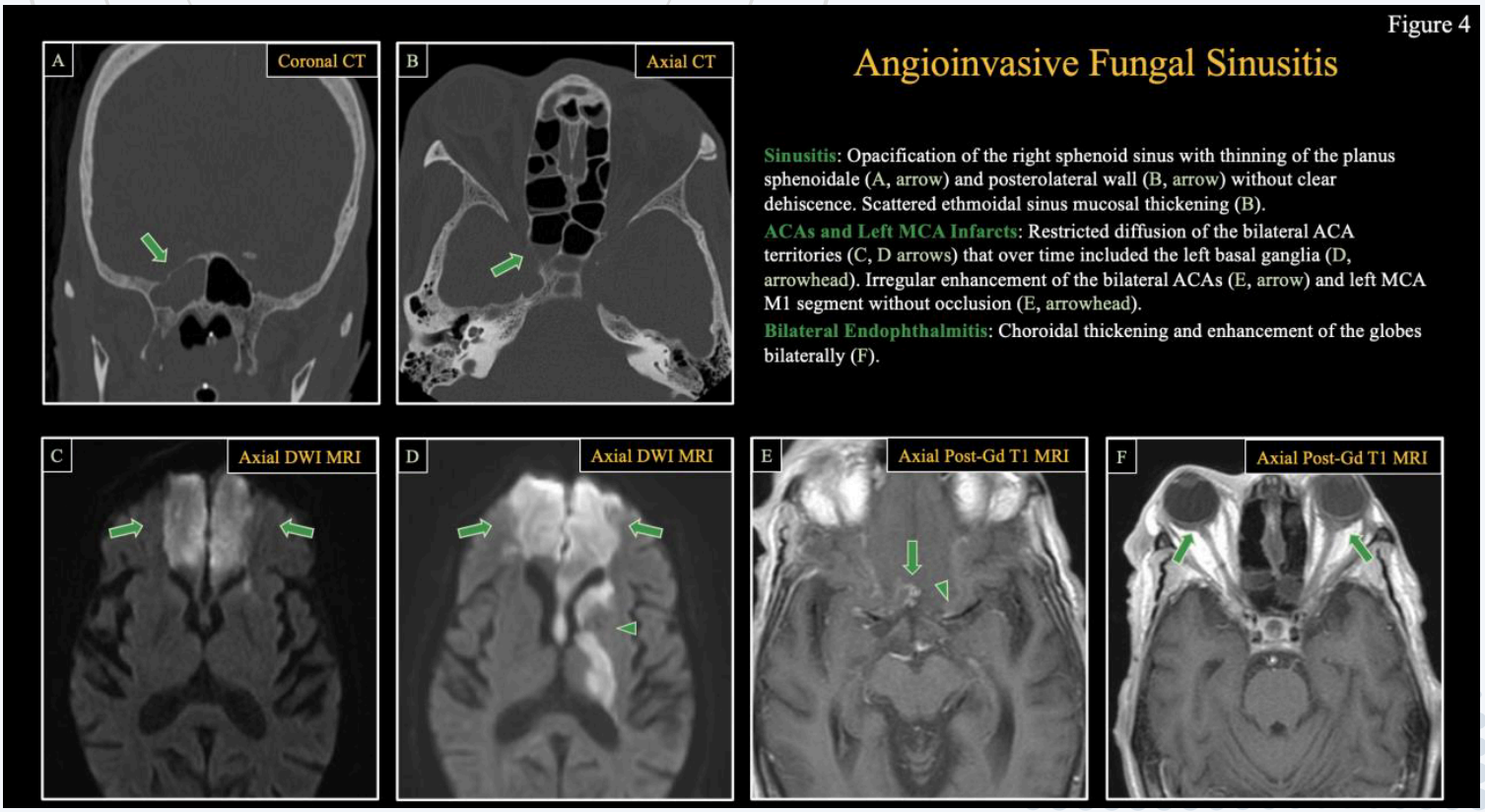

Figure 4 – Angioinvasive Fungal Sinusitis: 75-year-old female with a history of diabetes mellitus who presented with diabetic ketoacidosis and cardiogenic shock and was diagnosed with necrotizing invasive fungal sinusitis from sinus debridement surgical specimens with otolaryngology. Patient was also treated with intravenous antifungal medications and passed away while in hospice.

Conclusion:

Sinusitis can result in life-threatening intracranial complications and the radiologist is a key member of the multidisciplinary treatment team by identifying the cross-sectional imaging findings of sinusitis-related intracranial complications.

References:

Aribandi, M., McCoy, V. A., & Bazan III, C. (2007). Imaging features of invasive and noninvasive fungal sinusitis: a review. Radiographics, 27(5), 1283-1296.

Creemers-Schild, D., Gronthoud, F., Spanjaard, L., Visser, L. G., Brouwer, C. N., & Kuijper, E. J. (2014). Fusobacterium necrophorum, an emerging pathogen of otogenic and paranasal infections?. New Microbes and New Infections, 2(3), 52-57.

Dankbaar, J. W., van Bemmel, A. J. M., & Pameijer, F. A. Imaging findings of the orbital and intracranial complications of acute bacterial rhinosinusitis. Insights Imaging. 2015; 6 (5): 509-18.

Hallak, B., Bouayed, S., Ghika, J. A., Teiga, P. S., & Alvarez, V. (2022). Management Strategy of Intracranial Complications of Sinusitis: Our Experience and Review of the Literature. Allergy & Rhinology, 13, 21526575221125031.

Impact of a Collaborative Small Bowel Obstruction Imaging and Care Protocol with the General Surgery Service on Radiation Exposure and Resource Utilization

Authors: **Kaitlin M. Zaki-Metias, MD,** Mark Glover, DO, Trevena Metias, BSc, Nathaniel Sertu, BSc, Amy Braddock, MD, Bashir H. Hakim, MD, Stephen M. Seedial, MD

Trinity Health Oakland Hospital/Wayne State University School of Medicine, Pontiac, MI

Introduction:
Small bowel obstruction (SBO) is a common cause of diagnostic imaging, hospital admission, and surgical consultation. At our institution, following initial CT imaging without oral contrast demonstrating SBO, a second CT with oral contrast was typically obtained. A new protocol has been implemented in a collaboration between the department of surgery to eliminate the second CT, using oral Gastrografin® and serial abdominal radiographs for further assessment of SBO in clinically stable patients. This study aims to assess the impact of this protocol on radiation exposure and resource utilization.

Methods:
A retrospective cohort study was conducted on patients with SBO diagnosed on initial abdominopelvic CT for whom the general surgery service was consulted. Patients who underwent two abdominopelvic CT scans within 24 hours, one after the administration of oral contrast and one without, prior to implementation of the new protocol were selected for the control group. Ionizing radiation exposure, contrast media utilization, and CT technologist time were recorded for both groups.

Results:
Eighteen patients were included in the experimental group and 38 patients were included in the control group. Total effective dose (mSv) and CT technologist time were significantly less with the new protocol ($p=0.02$ and $p<0.001$, respectively). There was decreased use of intravenous contrast media in the experimental group relative to the control group, although this was not statistically significant ($p=0.06$).

Conclusion:
The implementation of a collaborative SBO imaging and care algorithm between general surgery and radiology resulted in reduced radiation exposure to patients and decreased CT technologist time.

Prognostic Value of MRI-Assessed Central Gland Volume for Biochemical Recurrence after Prostate Radiotherapy

Authors: **J. S. Lee**(1), K. Salari(1), S. R. Nandalur1, C. Shen(2), S. Al-Katib(23, L. Zhao(2), D. J. Krauss1, A. Thompson(1) Z. A. Seymour(1), and K. Nandalur(3)

1. Department of Radiation Oncology, Corewell Health William Beaumont University Hospital, Royal Oak, MI
2. Research Institute Biostatistics, Corewell Health William Beaumont University Hospital, Royal Oak, MI
3. Department of Radiology and Molecular Imaging, Corewell Health William Beaumont University Hospital, Royal Oak, MI

Objective:
Increasing central gland volume has been associated with less aggressive prostate cancer, theorized to be secondary to biomechanical stress from benign prostatic hyperplasia (BPH). The aim of this study was to evaluate pretreatment prostate magnetic resonance imaging (MRI) metrics and clinical characteristics in predicting biochemical recurrence (BCR) after definitive radiotherapy (RT) for prostate cancer.

Methods:
In this retrospective single institution study, we identified men in our database with National Comprehensive Cancer Network (NCCN) low, intermediate (IR), and high risk (HR) prostate cancer who underwent MRI within 6 months prior to completing definitive RT from May 2011 to February 2023. Total prostate volume, central gland volume, and peripheral zone volume were measured by a radiologist using manual segmentation, along with PI-RADS score. The primary objective was to determine the association of central gland volume with biochemical recurrence, defined by Phoenix criteria. Multivariable Cox proportional hazards regression model was constructed and adjusted for NCCN risk group, RT type, and MRI metrics.

Results:
A total of 373 men (median age 68 years, interquartile range [IQR] 62-73 years) were included, with a median follow-up of 28 months (IQR 16-43 months). 13 (3.5%) were low risk, 97 (26%) favorable intermediate risk (FIR), 201 (53.9%) unfavorable intermediate risk (UIR), and 62 (16.6%) high risk. 54 (14.5%) patients received conventionally fractionated RT, 105 (28.2%), moderately hypofractionated RT, 121 (32.4%), high-dose rate brachytherapy, and 93 (24.9%) stereotactic body RT. The 3 and 5 year rates of BCR were 7.8% and 18.3%, respectively. Taking into account NCCN risk group and RT type, higher central gland volume (per 5 cc) was associated with decreased risk of BCR (hazard ratio [HR]: 0.73, 95% confidence interval [CI]: 0.55-0.98, p=0.03). No significant association was seen with peripheral zone volume, PI-RADS score, or RT type. Relative to FIR, HR demonstrated increased risk of BCR (HR: 4.42, 95% CI: 1.04-18.8, p=0.04), while no association was seen with UIR.

Conclusion:
Increased central gland volume on pretreatment prostate MRI is independently associated with a lower risk of biochemical recurrence after definitive radiation for prostate cancer. BPH appears to confer favorable outcomes in RT patients and represent a novel, easily quantifiable metric in risk-stratification.

Rotationally Intensified Proton Lattice (RIPL): A Novel Method for Lattice Radiotherapy Utilizing Spot-Scanning Proton Arc

Authors: **J. S. Lee, D**. Mumaw, P. Liu, B. Loving, E. Sebastian, X. Ding, X. Cong, M. Stefani, B. Loughery, X. Li, R. L. Deraniyagala Jr, M. F. Almahariq, and T. J. Quinn

Department of Radiation Oncology, Corewell Health William Beaumont University Hospital, Royal Oak, MI

Objective:

The aim of this study is to explore the feasibility and dosimetric advantage of utilizing a spot-scanning proton arc approach (SPArc) for lattice radiotherapy in comparison with volumetric modulated arc therapy (VMAT) and intensity modulated proton therapy (IMPT) lattice techniques.

Methods:

Lattice plans were generated for 12 large tumors across abdomen, pelvis, lung, extremity, and head-and-neck sites using VMAT, IMPT, and SPArc techniques. Lattice geometries were standardized and algorithmically generated. Vertices were 1.5 cm in diameter and arrayed in a body-centered cubic lattice with a 6 cm lattice constant. Vertices were clipped within 0.5 cm of the target border or 1.5 cm of a critical Organ-At-Risk (OAR). Prescription dose was 20 Gy(RBE) in 5 fractions to the periphery of the tumor, with a simultaneous integrated boost (SIB) of 66.7 Gy(RBE) to the vertices. OAR constraints per AAPM TG-101 were prioritized. Dose Volume Histograms (DVH) were extracted and used to identify maximum, minimum, and mean doses; equivalent uniform dose (EUD); D95%, D50%, D10%, D5%; V19Gy; peak-to-valley dose ratio (PVDR); and gradient index (GI). Treatment delivery time of IMPT and SPArc were simulated based on the published DynamicARC model.

Results:

Median tumor volume was 591 cc with a median of 5 high-dose vertices per plan. Low dose coverage was maintained in all plans (median V19Gy: SPArc 95%, IMPT 95%, VMAT 95%). SPArc generated significantly greater dose gradients as measured by median PVDR (SPArc 3.91, IMPT 3.62, VMAT 3.02; SPArc-IMPT p=0.0005, SPArc-VMAT p=0.002) and high-dose GI (SPArc 6.9, IMPT 10.8, VMAT 12.3; SPArc-IMPT p=0.0005, SPArc-VMAT p=0.002). There was no significant difference in simulated treatment delivery time between SPArc and IMPT (p=0.31). OAR constraints were met in all plans.

Conclusion:

SPArc therapy was able to achieve high-quality lattice plans for various sites with superior gradient metrics (PVDR and GI) when compared to VMAT and IMPT. Clinical implementation of RIPL is warranted.

FDG-PET-based Selective De-escalation of Radiotherapy for HPV-Related Oropharynx Cancer: Results from a Phase II Trial

Authors: Samuel N. Regan*, Benjamin S. Rosen*, Krithika Suresh, Yue Cao, Madhava Aryal, Steven G. Allen, Kakit Wong, Keith A. Casper, Kelly M. Malloy, Mark E. Prince, Steven B. Chinn, Andrew G. Shuman, Molly Heft-Neal, Chaz Stucken, Chad Brenner, Paul L. Swiecicki, David A. Elliott, Jennifer L. Shah, Francis P. Worden†, Michelle L. Mierzwa†

Introduction:
Treatment de-escalation in HPV-related oropharyngeal squamous cell carcinoma (OPSCC) aims to minimize toxicity without compromising oncologic outcomes. We conducted a prospective phase II nonrandomized trial using FDG-PET imaging biomarkers to selectively de-escalate chemoradiotherapy (CRT). We hypothesized this would maintain locoregional control in all patients while decreasing toxicity in the de-escalated cohort.

Methods:
Eligible patients had stage I-II p16+ or HPV+ OPSCC with baseline tumor FDG-PET-avidity. All were planned to receive 70 Gy to gross disease and 56 Gy to elective nodal regions in 35 fractions with concurrent weekly carboplatin/paclitaxel. Mid-treatment PET was performed at fraction 10. If metabolic tumor volume was reduced by ⩾50%, CRT was completed at 54 Gy in 27 fractions.
The primary objective was to demonstrate non-inferiority of 24-month locoregional recurrence (LRR) overall by comparing the upper 90% confidence interval (CI) to 25%. Secondary objectives were failure patterns, survival, ctDNA trends, mpMRI, and toxicity. Toxicity measures included patient-reported outcomes (UWQOL-RTOG, FACT-HN, XQ). Kaplan-Meier analyses were used for survival outcomes.

R**esults:**
Eligible patients (n = 84) were enrolled from 2018 - 2023; 90% male, 75% stage I, and 48% never-smokers. De-escalation criteria were met in 42% (n = 35). The 54 Gy cohort had fewer patients with T3 tumors (3% vs 20%, p = 0.02) and lower median baseline weight (188 vs. 207 lbs, p = 0.015); no other differences in distribution of baseline factors nor initial RT plans were found.
Median follow up at this analysis was 28.9 mo overall, 31.6 mo for 54 Gy and 25.9 mo for 70 Gy patients. LRR at 24 mo was 7% (90% CI: 2% - 12.1%) in the entire cohort, 5% (90% CI: 0% - 10.5%) with 70 Gy, and 10% (90% CI: 1% - 18.2%) with 54 Gy. There were 5 LRR and 3 distant recurrences overall. Of 4 patients with only LRR, 3 were salvaged surgically without systemic therapy and have no evidence of disease, and 1 (70 Gy cohort) declined surgery. There was 1 cancer-related death after a distant-only recurrence in the 70 Gy cohort.

Median weight loss from baseline in the 54 Gy cohort was significantly less at 1 mo (6.5% vs. 10.6%, p <0.001) and 3 mo (6% vs. 12.6%, p <0.001) post-RT. Use of feeding tube during RT or ⩽1 mo post-RT was numerically better in 54 Gy patients (11% vs. 16%, p = 0.5). The 70 Gy cohort had one grade 4 (G4) carotid artery injury and one likely treatment-related death. The 54 Gy cohort had no G4+ toxicities, with less decrement from baseline in median UWQOL-RTOG scores for pain subscale at 1 mo (5 vs 10, p = 0.01) and mucus subscale at 12 mo (0 vs. 5, p = 0.2) post-RT. Remaining PRO instrument analyses are ongoing and will be presented.

Conclusion:
Mid-treatment FDG-PET may be a reliable biomarker to selectively de-escalate radiation dose in early-stage HPV+ OPSCC to improve toxicity while preserving oncologic outcomes.

Insights of Contemporary Diffusion MRI Modeling Techniques in Mild Traumatic Brain Injury: A TRACK-TBI Study

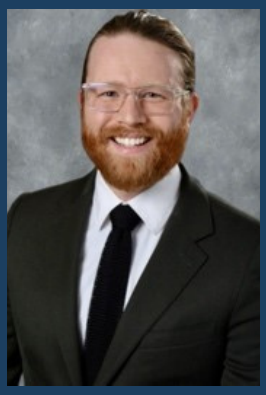

Authors: **Joshua H. Baker**1,2,3,4, Andrew Bender5, Norman Scheel1,4, David C. Zhu6, The TRACK-TBI Investigators.

1. Department of Radiology, Michigan State University
2. College of Osteopathic Medicine, Michigan State University
3. DO-PhD Physician Scientist Training Program, Michigan State University
4. Neuroscience Program, Michigan State University
5. Lou Ruvo Center for Brain Health, Cleveland Clinic
6. Department of Radiology, Albert Einstein College of Medicine

Introduction

The majority of traumatic brain injuries are categorized as mild (mTBI), and in up to 82% of cases, neuroimaging is ordered, with only ~9% of studies revealing intracranial pathology. Novel advanced neuroimaging techniques such as diffusion-weighted magnetic resonance imaging (DWI) are sensitive to subtle white matter changes following injury, but the natural history of these changes in recovery have yet to be fully defined. Inconsistencies in observed patterns of change with the common modeling technique diffusion tensor imaging (DTI) may be due to limitations of the model, and in this study, we explore novel modeling techniques that take advantage of high angular resolution multishell data collected during the TRACK-TBI study at UCSF.

Methods

DWI data at b-values of 1300 mm/s2 and 3000 mm/s2 from two-weeks and six-months post-injury were analyzed with MRtrix3's constrained spherical deconvolution and fixel-based analysis. Post-Hoc comparisons were conducted on white matter tracts constructed with TractSeg a deep learning algorithm trained on human connectome project data. Tract average metrics computed with DTI, diffusion kurtosis imaging (DKI), and neurite orientation dispersion and density imaging (NODDI) for projection fibers, long association fibers and commissural fibers were compared with fixel-based analysis metrics. The analysis scheme is summarized in Figure 1.

Results

Significant differences in all fixed-based metrics observed at the two-week timepoint remained at the six-month timepoint Figure 2. Differences between mTBI and control means decreased between timepoints, but a greater number of significant fixels were present for fiber density (FD), fiber cross-section (FC), and fiber density cross-section (FDC) at the six-month timepoint. There were no significant differences in any change images. Initially, a decrease in FD drove differences, whereas, at later time points, there was a greater contribution of decreased FC as well.

Conclusion

Fixel-based analysis revealed damage to white matter that was observed at two-weeks post mTBI remained at six-months post injury. This would suggest there is a difference in the time course of biological recovery and resolution of symptoms that should be the target of future study and interventions. Fixel-based analysis and NODDI metrics demonstrated similarities in sensitivity to white matter change, and there were no differences observed for the DTI metric FA. This adds further evidence it should not be used as the sole modeling technique when studying mTBI.

Segmental Agenesis of the Corpus Callosum with Pituitary Hypoplasia

Authors: Jake Haver MS-2, Joseph Junewick MD, FACR

Abstract:
Corpus callosum dysgenesis is found in 1:4000 individuals. Despite aberrant variations not being particularly rare, current research still aims at reconciling a mechanism for embryologic callosal development. It was once theorized that the corpus callosum develops linearly in a rostro-caudal direction from the genu to splenium - implying that focal absence of the body is due to an atrophic process. Since then, there has been increasing support for a theory that development occurs from multiple distinct foci, which later fuse. We describe a 3-year-old male with segmental agenesis of the corpus callosum, and provide neuroimaging in support of the latter theory. The patient is a 3-year-old male, born at 33 weeks. Pregnancy was complicated by maternal hypertension, BMI>50, and quarter pack-per-day cigarette use. The patient was admitted to the NICU with increased work of breathing, prolonged hypoglycemia, hypotension, and low free thyroxine with normal TSH. Further testing revealed an Insulin-like growth factor level of 37 ng/dL (15-150 ng/dL), a random growth hormone level of 0.91 ng/dL (<4.99 ng/dL), and a random cortisol level of 15.1 mcg/dL (3.0-22.0 mcg/dL). Testing excluded congenital adrenal hyperplasia. At an 8 week old evaluation with endocrinology, the patient passed an ACTH stimulation test, so further workup was not pursued. At 20 weeks, the patient underwent evaluation for episodic, non distractible, shuddering attacks, with an unremarkable EEG. At 45 weeks, the patient received a brainstem auditory evoked response test that was non-suggestive for hearing loss, despite concern on physical exam and at home. At 2 years and 11 months of age, the patient underwent evaluation for growth delay (length <3%, weight <10%). Insulin-like growth factor level was now 11 ng/dL (15-150 ng/dL.) Growth hormone response was tested via arginine/clonidine stimulation, and revealed severe growth hormone deficiency, prompting MRI evaluation of the pituitary gland. MRI of the brain revealed a Chiari I malformation (6mm displacement), a small pituitary gland (6.2 x 1.5 x 6.7mm) with infundibular thinning, and a complete absence of the callosal body despite full development of the genu and splenium. This case further endorses the association of midline commissural defects with pituitary hypoplasia, adds support to the theory of multifocal, alinear, corpus callosum development, and displays the futility of non-gestationally adjusted, isolated, pituitary hormone levels.

Optimizing Gallstone Management: Insights into Percutaneous Stone Removal Techniques

Presenter: Aliah McCalla, B.Eng - Medical Student, MS3, Central Michigan University
Author/Co-author: Pete Nesbitt, DO - Interventional Radiology Resident, Henry Ford Hospital
Author/Co-author: Shehbaz Shaikh, MD - Interventional Radiology Faculty, Henry Ford Health

Learning objectives:

- Recognize the role of percutaneous cholecystostomy tube (PCT) placement in high-risk acute cholecystitis patients.
- Understand the significance of pre-procedural abdominal CT imaging in tailoring gallstone removal procedures/device selection.
- Identify the techniques and devices used in gallstone removal, emphasizing the concept of combining approaches for safe and effective stone removal

Background:
The primary treatment for acute cholecystitis is cholecystectomy, but some high-risk patients may require PCT placement to alleviate the pressure behind the obstruction and drain bile temporarily. However, these tubes can lead to complications and may become permanent, especially if the patient is a poor surgical candidate at baseline. Lithotripsy, among other techniques, offers an alternative treatment to break up and remove the stones to facilitate tube removal, reducing complications and morbidity. Our poster presents an algorithm for gallstone removal in patients with PCTs and discusses some of the complications that can arise when using these devices.

Brief Clinical Findings/Procedural Details: A traditional pre-procedural assessment is used to determine a patient's suitability for stone removal. In addition to this traditional workup, abdominal CT imaging is essential to assess gallstone characteristics and plan the intervention path based on patient anatomy. After the characterization of the gallstone, an algorithmic approach can be used, with different approaches based on the number, size, and density of the stones for the appropriate next step. This will include devices such as disposable cholangioscope with electrohydraulic lithotripsy (EHL), nephoscope with dual-energy lithotripter, basket removal and irrigation with large sheath removal. While these devices have their own characteristics that make them advantageous, the ultimate best way for removal of the gallstones is a combination of the devices to create the optimal size and shape of the stone for removal from the patient. Additionally, as no procedure is without its complications, some complications can be minimized using the aforementioned pre-procedural evaluation. Regardless, complications do arise, including the well know risks such as biliary colic, leakage of bile, and infection such as bacteremia. Somewhat unique to stone removal is dislodgment of the stone into the common bile duct, resulting in choledocholithiasis, which may require additional interventions to manage.

Conclusion: In conclusion, chronic cholecystectomy tubes can significantly impact a patient's quality of life, emphasizing the need for alternative solutions when surgery is not an option. Lithotripsy offers a promising approach to help remove these tubes, relieving patients of this burden. It's important to recognize that the best treatment strategy may not be one-size-fits-all; instead, it often involves a combination of multiple techniques working together to safely remove the stones.

Orbital Foreign Bodies: What We Can See...

Presenter: Aliah McCalla, B.Eng, MD Candidate
Dr. Despoina Theotoka, MSc, MD
Dr. Michelle M. Maeng, MD
Dr. Michele H. Johnson, MD

Learning objectives:

- Recognize the role of percutaneous cholecystostomy tube (PCT) placement in high-risk acute cholecystitis patients.
- Understand the significance of pre-procedural abdominal CT imaging in tailoring gallstone removal procedures/device selection.
- Identify the techniques and devices used in gallstone removal, emphasizing the concept of combining approaches for safe and effective stone removal

Summary:
Blunt and penetrating trauma to the orbit is a common cause of emergency ophthalmologic evaluation, imaging and treatment. These patients will often present with pain, discomfort, bleeding or visual loss. Frequently physical evaluation for extent of injury is challenging. Emergency imaging is leveraged to diagnose extent and pattern of orbital injury. Precise anatomic delineation of the imaging pattern of orbital injury includes careful scrutiny for orbital foreign bodies. Orbital foreign bodies may lead to globe rupture, vision loss, infection and retinal toxicity. Imaging plays a critical role in injury assessment and development of effective treatment plan.

Purpose:
The purpose of this educational exhibit is to review the clinical and radiologic anatomy of blunt and penetrating orbital injuries with a focus on identification of orbital foreign bodies which may determine the need for surgical treatment. The foreign body composition may include wood, glass, metal, bone fragments among other more unusual materials.

Materials and Methods:
Retrospective clinical and teaching cases are utilized to demonstrate anatomic patterns of injury as well as subtle and unmistakable orbital foreign bodies. Characterization of the type of foreign body through the use of clinical images, plain films, CT and MRI is demonstrated through real world examples. Imaging features to differentiate various materials will be highlighted. Results and Conclusions: Multiple case examples of blunt and penetrating orbital trauma are presented each containing a foreign body. Wood, glass, metal, including BBs and bullets and unusual penetrating objects such as pens and pencils, fish hooks and lawn darts have been reported. While some inert materials may be safely left in place without consequence, others may present an ongoing risk of infection or toxicity to orbital structures. Meticulous imaging can assist the ophthalmologist in the assessment of the extent of orbital injury and to determine optimal management for preservation of function.

Educational objectives:
• Overview the anatomy of the orbit in the setting of trauma
• Discuss the predominant forms of foreign bodies to the orbit
• Discuss how to distinguish between different forms of foreign bodies to the orbit via imaging
• Review the risks of intraorbital foreign bodies including globe rupture, infection and visual loss
• Discuss the different treatment plans for foreign bodies to the orbit

Contrast Reflux During Catheter-Directed Embolectomy: Significance for Extracorporeal Membrane Oxygenation in High-Risk Pulmonary Embolism

Syed Raza1, Younes Jahangiri MD2,3
1. College of Human Medicine, Michigan State University, Grand Rapids, MI
2. Division of Interventional Radiology, Corewell Health West Michigan, Grand Rapids, MI
3. Department of Radiology, College of Human Medicine, Michigan State University, Grand Rapids, MI

Email addresses of authors: Syed Raza(razasye3@msu.edu), Younes Jahangiri(younes.jahangirinoudeh@corewellhealth.org)

Case Report:
A 74-year-old female with a past medical history of hypertension and symptomatic anemia presented to the emergency department (ED) with chief complaints of generalized weakness and dyspnea. Computed tomography (CT) angiography of the thorax with contrast demonstrated extensive bilateral pulmonary emboli(PE) with acute right heart strain (right ventricle (RV)/left ventricle (LV) ratio: 2.4) (Figure.1, red arrows). The decision was made to pursue catheter guided thrombectomy. Initial contrast injection through the right femoral venous sheath showed retrograde reflux of contrast into the left iliac venous system as well as poor antegrade flow in the inferior vena cava (IVC) suggestive of impaired right ventricular function (Figure 2a,2b,2c,2d, red arrows). Intraprocedurally, the patient experienced cardiac arrest, and following 30 minutes without return of shockable activity, the code was terminated. The patient was pronounced deceased.

Discussion:
The use of Extracorporeal Membrane Oxygenation (ECMO) in the management of high-risk PE has gained traction in recent years, with the 2019 American Heart Association (AHA) and 2019 European Society of Cardiology (ESC) statements suggesting that patients requiring surgical embolectomy or catheter-directed treatment may benefit from ECMO support to prevent periprocedural collapse, if not otherwise contraindicated (e.g., severe aortic valve regurgitation, severe neurologic impairment, liver cirrhosis, etc.) [1]. Guidelines for ECMO initiation are unclear at this time due to limited studies identifying patients who would benefit from this intervention, as well as appropriate timing [2]. This case highlights the significance of access site contrast reflux to the contralateral iliac vein as a potential marker for severe RV failure, prompting consideration for ECMO intervention.

Patient risk stratification could aid in establishing ECMO guidelines for high-risk patients, especially those undergoing catheter directed therapies and thrombolytic contraindications. Moreover, the formation of an ECMO multidisciplinary team placed on standby for high-risk PE patients plays a pivotal role. This approach aims to eliminate emergent ECMO cannulation scenarios as well as possibly securing percutaneous arterial and venous femoral access prior to intervention and maintaining for a designated duration post-intervention [3].

References:
1 Konstantinides SV, Meyer G, Becattini C, et al. 2019 ESC Guidelines for the diagnosis and management of acute pulmonary embolism developed in collaboration with the European Respiratory Society (ERS). Eur Heart J. 2020;41(4):543-603. doi:10.1093/eurheartj/ehz405
2 Boey JJE, Dhundi U, Ling RR, Chiew JK, Fong NC-J, Chen Y, Hobohm L, Nair P, Lorusso R, MacLaren G, et al. Extracorporeal Membrane Oxygenation for Pulmonary Embolism: A Systematic Review and Meta-Analysis. Journal of Clinical Medicine. 2024; 13(1):64. doi: 10.3390/jcm13010064
3 TJ, Sheasby J, Sawhney R, et al. Extracorporeal membrane oxygenation for large pulmonary emboli. Proc (Bayl Univ Med Cent). 2023;36(3):314-317. Published 2023 Feb 9. doi:10.1080/08998280.2023.2171699

Figure 1: Extensive bilateral pulmonary emboli (red arrows) with RV/LV ratio of 2.4

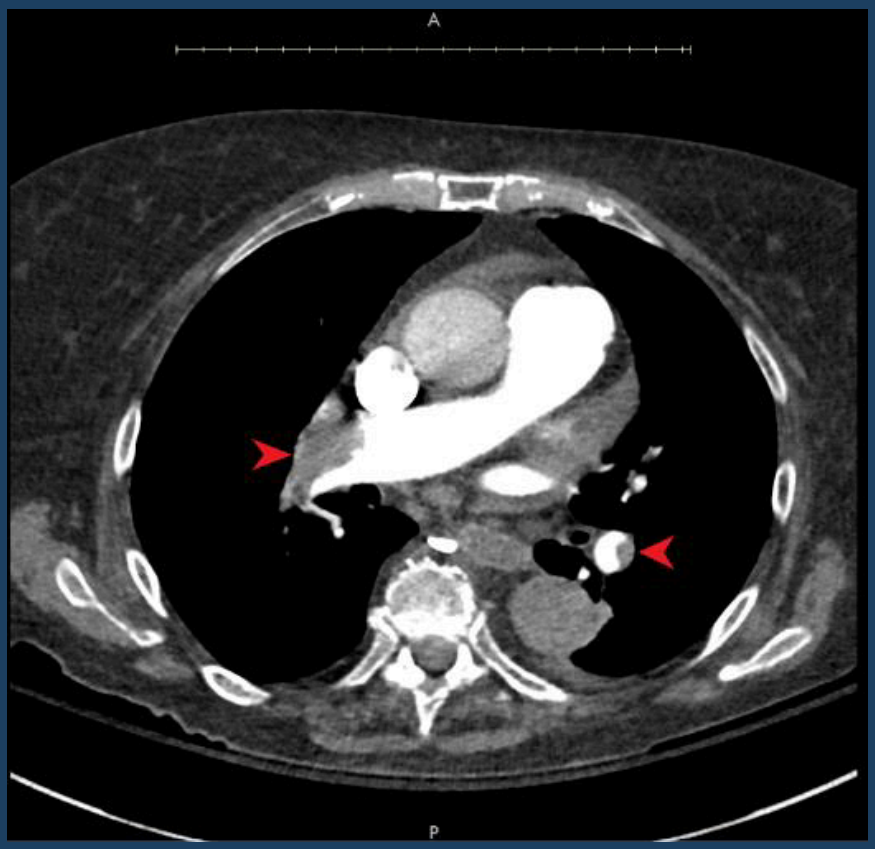

Figure 2 (a,b,c,d): Retrograde reflux of contrast into the left iliac vein (red arrows)

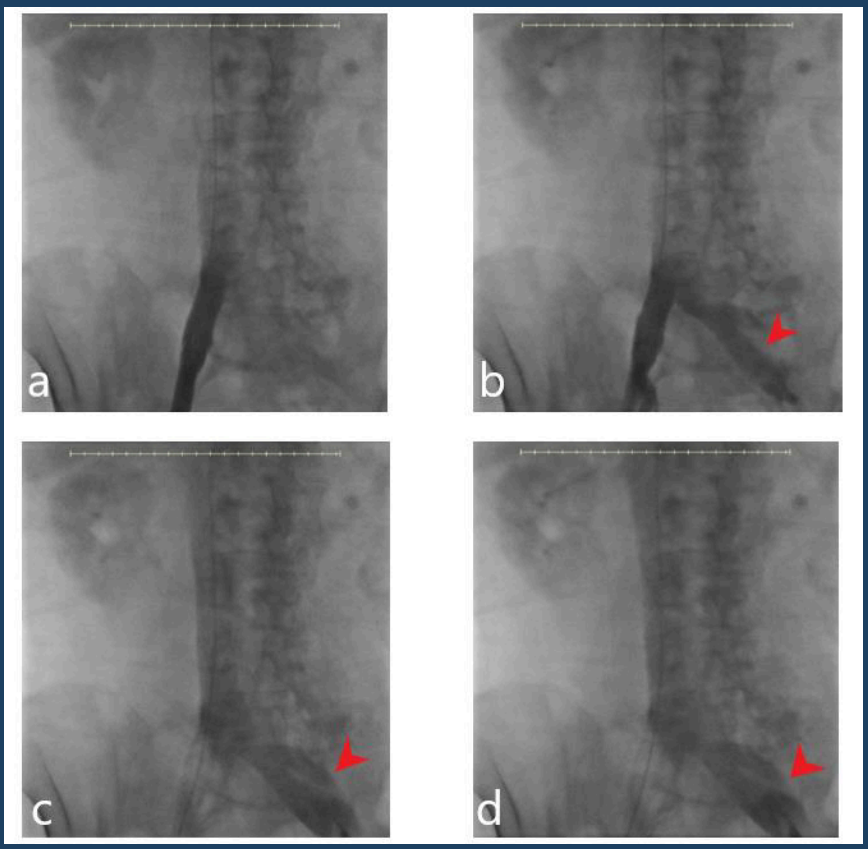

Ovarian Cancer (OC) Remains a Leading Gynecological Cancer with High Mortality.

Cody Townsley OMS-III, and Khaleel Quasem MS-IV.

Introduction:
Ovarian Cancer (OC) remains a leading gynecological cancer with high mortality. Therapeutic intervention is difficult due to advanced disease and complex metastasis at diagnosis. Tumor debulking remains the primary intervention, however residual tumor often remains undetected within the peritoneal cavity due to absence of intraoperative tumor-detection

Imethods. Radiotheranostics is a rapidly growing modality in treating similar metastatic disease, yet inadequate radiobiological studies hinder establishing new standard of care treatments. Therefore, novel methods of intraperitoneal (IP) tumor detection are necessary.

Methods:
Our lab has established a peptide-based OC targeted methodology, successfully implemented in rodents, ready for translational studies in Large Animals (LA). However, robust LA models of OC are absent from the field. We propose a method for LA models of human OC using excised human OC xenografted into immunocompetent models. LA models are comparable to human models of metastatic disease in many facets, thus findings will further efforts in earlier detection and provide a model of metastatic IP disease. Establishing our animal model has been completed in steps, validating the progression for subsequent study and now, use of extracted human tissue. First, characterization of targeted moieties of human OC cells was conducted in small animal models (SA). SKOV-3 Luciferase+ OC cells (SKOV-3) were injected into SA peritoneal cavities. Tumor burden was monitored for four weeks using In Vivo Imaging System Bioluminescence (IVIS-BLI) followed by image guided surgical excision. Specimens were fixed in formalin after ex-vivo incubation in artificial IP solution at 0-, 1-, 2-, and 4-hour post-excision times. Tumor stability was measured through histo-analysis expression of OC antigens Claudin 3 and 4, and folate receptor.

Results:
Tumors were found to show increasing growth throughout the 4 weeks and positive OC surgical extraction occurred in 100% (9/9) mice who received SKOV-3 IP injection. Histological analysis confirmed the integrity of tumor targeting moieties in all time frames with Claudin 3 showing the greatest viability. Subsequently, tumors were grown in SA models, xenografted into larger SA models, then excised and analyzed at 1- and 2- hour time points. Results of this study were inconclusive.

Conclusion:
Currently, pending IRB approval, extracted human OC tissue will be xenografted into LA models and analyzed for tissue viability. We hypothesize there may be a time-sensitive window for study after excision of metastatic OC. This window has been established as at least 4 hours in ex-vivo studies. In-vivo SA xenograft results could mean this time window is less than previously expected, heavily influenced by recipient immune system, or other factors. With human to LA (pig) xenograft studies, we aim to characterize these influences. Such studies will allow for in-vitro OC antigen specific radioisotope labeled detection and eventual pharmacotherapy.

Recovery and Adaptation: Radiology Volumes Post-Pandemic Using Data from 12.4 Million Imaging Examinations, 197 Facilities, and 1,600 Radiologists

First Name		Last Name	Email	Role	Affiliation
Haniyeh		Zamani	hzamani@wayne.edu	1st author	Wayne State University School of Medicine
Tom		Fruscello	tfruscello@acr.org	Co-author	ACR
Mythreyi		Chatfield	mchatfield@acr.org	Co-author	ACR
Judy		Burleson	JBurleson@acr.org	Co-author	ACR
Mike		Simanowith	msimanowith@acr.org	Co-author	ACR
Abe		Fernandez	afernandez@acr.org	Co-author	ACR
Matthew		Davenport	matdaven@med.umich.edu	Senior Author	Michigan Medicine Departments of Radiology and Urology

Introduction:

The COVID-19 pandemic transformed radiology and had a dramatic effect on radiology imaging volumes. This study aims to analyze the changes in imaging volumes across a diverse sample of radiology facilities in the United States before, during, and after the COVID-19 pandemic.

Methods:

We conducted a comprehensive analysis of imaging volumes from 197 radiology facilities and 1,600 radiologists across 23 states in the United States (academic [N<=5], community hospital [N=79], multi-specialty clinic [N<=5], freestanding imaging center [N=109], other [N<=5]). Data from 12.4 million imaging examinations were collected from December 1, 2017, to February 28, 2023, covering the pre-pandemic, pandemic, and post-pandemic periods. Six modalities—computed tomography (CT), mammography, magnetic resonance imaging (MRI), X-ray, ultrasound, and positron emission tomography (PET)-CT—were assessed individually and collectively. Using the American College of Radiology (ACR) General Radiography Improvement Database (GRID), we tracked changes in workforce number, workload, NPI attrition, and NPI turnover by quarter, utilizing National Provider Identifiers (NPIs) to identify individual radiologists.

Results:

Of the 1,600 radiologists, 804 (50%) remained throughout the study period, with 581 (36%) consistently reading at least 100 examinations per quarter in included practices. The average change in exams read per day from 2017 to 2023 was +1.4% (49.5/day to 50.9/day) and -0.2% (54/day to 53.8/day), indicating a complete recovery following a peak decline of -35%/quarter (2,015,150 to 1,304,748) in March through May 2020. Notably, radiologists in the top quartile of productivity experienced significant increases in exams read per day (+25.4%; 52.3/day baseline vs. 65.6/day in 2022) and clinical days worked per quarter (+24.4%; 37.7 vs. 46.9, respectively) from 2017 to 2022. Despite considerable turnover, the number of unique radiologists in the sample increased from 997 (baseline) to 1,144 (2023), with days worked per national provider identifier number (NPI) per quarter remaining relatively stable (40 days vs. 39 days).

Conclusion:

Our findings indicate a complete recovery of radiology imaging volume post-pandemic. While the average radiologist's workload remained similar pre- and post-pandemic, high-volume radiologists exhibited a 25% increase in examinations read per day and worked 24% more clinical shifts per quarter. These insights highlight the adaptability and resilience of radiology practices in responding to the challenges posed by the COVID-19 pandemic.

THANK YOU TO OUR SPONSORS!